



QUANTUM CHAOS FOR THE VIBRATING RECTANGULAR BILLIARD

MASON A. PORTER and RICHARD L. LIBOFF

*Center for Applied Mathematics and
Schools of Electrical Engineering and Applied Physics,
Cornell University, Ithaca, NY 14850, USA*

Received July 21, 2000; Revised November 3, 2000

We consider oscillations of the length and width in rectangular quantum billiards, a two “degree-of-vibration” configuration. We consider several superposition states and discuss the effects of symmetry (in terms of the relative values of the quantum numbers of the superposed states) on the resulting evolution equations and derive necessary conditions for quantum chaos for both separable and inseparable potentials. We extend this analysis to n -dimensional rectangular parallelepipeds with two degrees-of-vibration. We produce several sets of Poincaré maps corresponding to different projections and potentials in the two-dimensional case. Several of these display chaotic behavior. We distinguish between four types of behavior in the present system corresponding to the separability of the potential and the symmetry of the superposition states. In particular, we contrast harmonic and anharmonic potentials. We note that vibrating rectangular quantum billiards may be used as a model for quantum-well nanostructures of the stated geometry, and we observe chaotic behavior without passing to the semiclassical ($\hbar \rightarrow 0$) or high quantum-number limits.

1. Introduction

Quantum billiards have been studied extensively in recent years. These systems describe the motion of a point particle undergoing perfectly elastic collisions in a bounded domain with Dirichlet boundary conditions. Blümel and Esser [1994] observed quantum chaos in the one-dimensional vibrating quantum billiard. Porter and Liboff [2001b] extended these results to a class of quantum billiards with one *degree-of-vibration* (*dov*). They found necessary conditions for chaotic behavior to occur in such billiards in addition to the general form of the equations describing the dynamics of two superposition states in one *dov* quantum billiards. One of the goals of this paper is to explore a generalization of these results by considering a two *dov* billiard system. The present paper thereby accomplishes two things. First, it expands the theory of quantum chaos by analyzing billiard systems with more than

one *dov*. Second, it offers a model for quantum-well nanostructures of rectangular geometry.

In the present paper, we consider vibrations with two degrees-of-freedom in rectangular quantum billiards. We consider several superposition states and discuss the effects of symmetry on the equations of motion produced. We extend this analysis to n -dimensional rectangular parallelepipeds with two degrees-of-vibration. We produce several sets of Poincaré maps corresponding to different projections and potentials that display chaotic behavior for the two-dimensional case. We distinguish between four cases corresponding to the separability of the billiard potential and the symmetry of the superposition states. In particular, we contrast harmonic and anharmonic oscillators. Lastly, we note that the present analysis does not require passage to the semiclassical ($\hbar \rightarrow 0$) or high quantum-number limits, as is commonly believed to be necessary in the study of quantum chaos [Gutzwiller, 1990].

2. Statement of the Problem

The rectangular quantum billiard problem addresses the system of a point particle of mass m undergoing perfectly elastic collisions inside a rectangular well. The vertices of the rectangle are at $(-a/2, -b/2)$, $(-a/2, b/2)$, $(a/2, -b/2)$, and $(a/2, b/2)$. If a and b are independent of time — that is, if we consider the zero *dov* problem — a solution of the Schrödinger equation is given by the following superposition of eigenstates:

$$\psi(x, y, t) = \sum_{n_x=1}^{\infty} \sum_{n_y=1}^{\infty} \alpha(a, b) A_{n_x n_y} \psi_{n_x n_y}(x, y) \times \exp\left[-\frac{iE_{n_x n_y} t}{\hbar}\right], \tag{1}$$

where $A_{n_x n_y}$ represents the (complex) amplitude of the state with quantum numbers (n_x, n_y) , $E_{n_x n_y} \equiv \varepsilon_a(n_x) + \varepsilon_b(n_y)$ is the $n_x n_y$ th eigenenergy, and $\psi_{n_x n_y}$ is the corresponding eigenstate of the system, given by

$$\psi_{n_x n_y}(x, y) = \psi_{n_x}(x) \psi_{n_y}(y), \tag{2}$$

where

$$\psi_l(w) = \cos\left(\frac{\pi l w}{q}\right) \tag{3}$$

if l is even and

$$\psi_l(w) = \sin\left(\frac{\pi l w}{q}\right) \tag{4}$$

if l is odd. We absorb the $n_x n_y$ th (time-dependent) phase

$$\exp\left[-\frac{iE_{n_x n_y} t}{\hbar}\right] \tag{5}$$

into the coefficient $A_{n_x n_y}$ as in [Porter & Liboff, 2001b]. In the above equations, note that for the length $w = x$, $l = n_x$ and $q = a$, and for the width, $w = y$, $l = n_y$ and $q = b$. Additionally,

$$\alpha(a, b) = \frac{2}{\sqrt{ab}} \tag{6}$$

represents the normalization for the state with quantum numbers (n_x, n_y) .

Allowing the walls to vibrate corresponds to a and b depending on time and $A_{n_x n_y}$ having a time-dependence other than the phase factor (5). All other parameters in the above equations remain constant with respect to time.

In the two *dov* rectangular quantum billiards, one has a rectangular-well potential with movable walls described by its length $a(t)$ and width $b(t)$. The kinetic energy of the confined particle is given by

$$K = -\frac{\hbar^2}{2m} \nabla^2, \quad x \in \left[-\frac{a(t)}{2}, \frac{a(t)}{2}\right], \tag{7}$$

$$y \in \left[-\frac{b(t)}{2}, \frac{b(t)}{2}\right],$$

where m is the mass of the confined particle and the Laplacian ∇^2 is represented in Cartesian coordinates. The Hamiltonian for the entire system is given by

$$H(a, P_a, b, P_b) = K + \frac{P_a^2}{2M_a} + \frac{P_b^2}{2M_b} + V(a, b), \tag{8}$$

where

$$P_a = -i\hbar \frac{\partial}{\partial a} \tag{9}$$

is the momentum of the horizontal walls (which have mass $M_a \gg m$), and

$$P_b = -i\hbar \frac{\partial}{\partial b} \tag{10}$$

is the momentum of the vertical walls (which have mass $M_b \gg m$). The billiard boundary moves in a potential $V(a, b)$. Note that the Hamiltonian (8) consists of both a classical component ($P_a^2/2M_a + P_b^2/2M_b$) and a quantum one ($K + V$). In the present paper, we utilize the Born–Oppenheimer approximation [Blümel & Esser, 1994] in using only the quantum-mechanical component of the Hamiltonian in the Schrödinger equation. This scheme is often used in systems that have both a slow (classical) and fast (quantum) component, and it is a common approximation in mesoscopic physics. In the present analysis, we will also be ignoring geometric phases [Zwanziger *et al.*, 1990].

3. Special Cases: Reduction to One Degree-of-Vibration

If either the length $a(t)$ or the width $b(t)$ (but not both) is independent of time, then the present problem reduces to the one-dimensional vibrating quantum billiard [Blümel & Esser, 1994; Blümel & Reinhardt, 1997]. Either P_a or P_b vanishes identically, so this corresponds exactly to the one-dimensional vibrating billiard. The general form

of such one *dov* quantum billiards was established recently [Porter & Liboff, 2001b].

If $a(t) = b(t)$ for all time, the rectangular quantum billiard is constrained to be a square. By considering the diagonal, one obtains a single *dov* problem, as the motion of the boundary is described by the motion along a single dimension. The analysis of the problem is similar to but not precisely the same as previous analyses of one *dov* quantum billiards [Porter & Liboff, 2001b; Liboff & Porter, 2000]. The difference lies in the fact that in a superposition state, one may consider different levels of excitation in the length and width. One cannot directly apply the theorems on one *dov* quantum billiards derived by Porter and Liboff [2001b], because the vibrating dimension does not correspond to one of the dimensions obtained using separation of variables. In other words, this procedure results in coordinates with which we cannot satisfy the global separability requirement of those theorems. (That is, the geometry of the boundary does not correspond precisely to the geometry we would have to use in the separation of variables procedure in this case.) Hence, even though the problem reduces to a one *dov* problem, one cannot apply previous theorems derived for that situation because one does not have global separability in the diagonal coordinates in a square quantum billiard. (It is likely, however, that a generalization of those theorems can be applied.)

For a rectangular geometry, one obtains variables corresponding to the length and width when using separation of variables to solve the stationary Schrödinger (Helmholz) equation. To apply the cited theorems directly, one needs a basis of quantum numbers that correspond to these dimensions. The dimensions in question in the present case are parallel to the vectors $\hat{x} + \hat{y}$ and $\hat{x} - \hat{y}$, where \hat{x} and \hat{y} are unit vectors parallel to the x and y axes, respectively. In order to apply these theorems, one would first have to check if the Helmholtz equation is separable using this geometric configuration. Applying the boundary conditions in the present situation is more complicated because of the different geometries of the boundary and the variables. (The boundaries have a nontrivial functional dependence on the variables. Define $x' \equiv x + y$ and $y' \equiv x - y$. Applying Dirichlet boundary conditions requires solving $\psi(1/2[x' + y'], 1/2[x' - y'] = \pm a) = 0$ for all (x', y') and $\psi(1/2[x' + y'] = \pm a, 1/2[x' - y']) = 0$ for all (x', y') . It is simpler to obtain results for the

vibrating square billiard directly as a special case of the vibrating rectangular quantum billiard.)

One can generalize this idea of geometric constraints and the *dov* of a quantum billiard. Of course, as is the case with the vibrating square above, this procedure does not in general preserve global separability in a manner easily applied so one has to be careful about applying known theorems for one *dov* quantum billiards. This caveat aside, consider as an example the vibrating ellipsoidal quantum billiard with major and minor axes with characteristic radii $a_1(t)$, $a_2(t)$, and $a_3(t)$. If the eccentricities of the ellipse are constrained to be constants, then this billiard has a single *dov*. If one eccentricity (e.g. that relating $a_1(t)$ and $a_2(t)$ so that $a_1(t) = a_2(t)\sqrt{1 - e_{12}^2}$ for a constant eccentricity e) is constrained to be constant but the others are not so that $a_3(t)$ is independent of the other two radii, the billiard has two *dov*. If all three radii are permitted to vary independently, then the billiard has three *dov*. The radially vibrating spherical billiard is the special case of this example in which $a(t) \equiv a_1(t) = a_2(t) = a_3(t)$ (since the eccentricities $e_{12} = e_{13} = e_{23} \equiv 0$). It has only one *dov* precisely because it is constrained to vibrate in the radial direction [Liboff & Porter, 2000]. If angular vibrations are permitted in the spherical billiard, then there are additional degrees-of-vibration corresponding to the fact that the billiard has fewer geometric constraints.

4. Equations of Motion

Consider a two-state superposition of a two *dov* quantum billiard, so that

$$\begin{aligned} \psi(x, y, t) = & A_1(t)\alpha(a(t), b(t))\psi_{n_x n_y}(x, y, t) \\ & + A_2(t)\alpha(a(t), b(t))\psi_{n'_x n'_y}(x, y, t), \end{aligned} \quad (11)$$

which we may write using Dirac notation [Sakurai, 1994] as

$$|\psi\rangle = \psi_1|n_x n_y\rangle + \psi_2|n'_x n'_y\rangle. \quad (12)$$

We note that even in the special case of the square, the states corresponding to the length and width need not have the same level of excitation despite the fact that we impose the constraint $a(t) \equiv b(t)$. That is, some outside force imposes the constraint, so a different level of excitation in the length and

width does not cause the square to deform into a rectangle. Equivalently, the eigenstates may be excited separately in the variables x and y , even though the Hamiltonian for the vibrating square billiard has one degree-of-vibration.

The time-dependent Schrödinger equation for the present system is

$$i\hbar \frac{\partial \psi(x, y, t)}{\partial t} = -\frac{\hbar^2}{2m} \nabla^2 \psi(x, y, t), \tag{13}$$

$$x \in \left[-\frac{a(t)}{2}, \frac{a(t)}{2} \right], \quad y \in \left[-\frac{b(t)}{2}, \frac{b(t)}{2} \right],$$

where the kinetic energy K of the particle confined within the billiard is as before and the total Hamiltonian of the system is given by

$$H = K(a, b) + \frac{P_a^2}{2M_a} + \frac{P_b^2}{2M_b} + V, \tag{14}$$

where the walls of the quantum billiard have momenta P_a and P_b conjugate (respectively) to the length a and width b . These walls have respective masses M_a and M_b and move in a potential

$$V = V(a, b), \tag{15}$$

which is assumed to not have any explicit time-dependence.

Inserting the two-term superposition into the Schrödinger equation (13) and taking expectations gives the following relations:

$$\begin{aligned} \left\langle \psi \left| -\frac{\hbar^2}{2m} \nabla^2 \psi \right. \right\rangle &= \frac{1}{a^2} (\varepsilon_a^{(1)} |A_1|^2 + \varepsilon_a^{(2)} |A_2|^2) \\ &\quad + \frac{1}{b^2} (\varepsilon_b^{(1)} |A_1|^2 + \varepsilon_b^{(2)} |A_2|^2), \tag{16} \\ i\hbar \left\langle \psi \left| \frac{\partial \psi}{\partial t} \right. \right\rangle &= i\hbar [\dot{A}_1 A_2^* + \dot{A}_2 A_1^* + \nu_{11} |A_1|^2 \\ &\quad + \nu_{22} |A_2|^2 + \nu_{12} A_1 A_2^* + \nu_{21} A_2 A_1^*], \end{aligned}$$

where ν_{ij} are the coefficients of the quadratic form. In Eq. (16),

$$\begin{aligned} \varepsilon_a^{(1)} &\equiv \frac{(n_x \pi \hbar)^2}{2m}, & \varepsilon_a^{(2)} &\equiv \frac{(n'_x \pi \hbar)^2}{2m}, \\ \varepsilon_b^{(1)} &\equiv \frac{(n_y \pi \hbar)^2}{2m}, & \varepsilon_b^{(2)} &\equiv \frac{(n'_y \pi \hbar)^2}{2m}. \end{aligned} \tag{17}$$

Recall that the energy $E_{n_x n_y}$ of the $n_x n_y$ th eigenstate is given by

$$E_{n_x n_y} = \varepsilon_a^{(1)} + \varepsilon_b^{(1)} \tag{18}$$

The assumption of a two-term superposition state corresponds to a two-term Galérkin projection, an idea that has been used in fluid mechanics and finite-element numerical methods [Guckenheimer & Holmes, 1983; Temam, 1997; Johnson, 1987]. This method is used to analyze the dynamics of partial differential equations approximately using a system of ordinary differential equations. Note that if one considers a superposition of every possible state in the above procedure, one obtains an infinite set of coupled ordinary differential equations exactly describing the dynamics of the full system. One thus applies a finite-dimensional projection in order to both make the subsequent analysis tractable and to isolate the effects of particular eigenstates. Which two eigenstates one considers in a two-term superposition determines the values of the coupling coefficients μ_{jk} , which are defined by the relation

$$\nu_{jk} \equiv \mu_{jk} \frac{\dot{a}}{a} \quad \text{or} \quad \nu_{jk} = \mu_{jk} \frac{\dot{b}}{b} \quad (\text{see Theorem 1}). \tag{19}$$

Analogous to the radially vibrating spherical quantum billiard [Liboff & Porter, 2000], the dynamical behavior of the present system depends in a fundamental manner on whether these coefficients vanish. By computing the expectations above and recalling orthogonality relations of harmonic functions, we obtain the following result:

Theorem 1. *The coefficients μ_{jk} and μ_{kj} , ($j \neq k$) for a superposition of two eigenstates in the two dov rectangular quantum billiard do not vanish if and only if either $n_x = n'_x$ or $n_y = n'_y$. The coefficients μ_{jj} and μ_{kk} always vanish, and the relation $\mu_{jk} = -\mu_{kj}$ always holds. Moreover, ν_{jk} is proportional to \dot{a}/a if $n_y = n'_y$ and to \dot{b}/b if $n_x = n'_x$. This proportionality constant is exactly as in the one-dimensional vibrating quantum billiard. Using the indices n and n' to represent either the pair (n_x, n'_x) or (n_y, n'_y) corresponding to which of the two pairs has distinct values and also taking $n < n'$ without loss of generality gives the coupling coefficient*

$$\mu_{jk} \equiv \mu_{nn'} = \frac{2nn'}{(n' + n)(n' - n)}. \tag{20}$$

If considering a superposition of more than two states, this theorem applies pairwise. If the billiard resides in a “separable” potential such as the harmonic potential, it has parameter regions in which

it behaves chaotically if and only if the coupling coefficient is nonzero.

The above theorem is a statement of the necessary and sufficient conditions for a two *dov* quantum billiard in a separable potential to exhibit chaos. (If the billiard resides in an “inseparable” potential, however, we will show that it can behave chaotically even if the coupling coefficient vanishes.) In particular, Theorem 1 implies that a two *dov* rectangular quantum billiard has only four types of two-term superpositions that give nonvanishing cross terms μ_{jk} and μ_{kj} . (This follows from orthogonality conditions and the application of trigonometric identities.) These are

$$\begin{aligned} \psi &= A_1 \alpha \cos\left(\frac{n_x \pi x}{a}\right) \cos\left(\frac{n_y \pi y}{b}\right) \\ &\quad + A_2 \alpha \cos\left(\frac{n'_x \pi x}{a}\right) \cos\left(\frac{n'_y \pi y}{b}\right), \\ \psi &= A_1 \alpha \cos\left(\frac{n_x \pi x}{a}\right) \sin\left(\frac{n_y \pi y}{b}\right) \\ &\quad + A_2 \alpha \cos\left(\frac{n'_x \pi x}{a}\right) \sin\left(\frac{n'_y \pi y}{b}\right), \\ \psi &= A_1 \alpha \sin\left(\frac{n_x \pi x}{a}\right) \cos\left(\frac{n_y \pi y}{b}\right) \\ &\quad + A_2 \alpha \sin\left(\frac{n'_x \pi x}{a}\right) \cos\left(\frac{n'_y \pi y}{b}\right), \\ \psi &= A_1 \alpha \sin\left(\frac{n_x \pi x}{a}\right) \sin\left(\frac{n_y \pi y}{b}\right) \\ &\quad + A_2 \alpha \sin\left(\frac{n'_x \pi x}{a}\right) \sin\left(\frac{n'_y \pi y}{b}\right), \end{aligned} \tag{21}$$

where in each of the above equations, either $n_x = n'_x$ or $n_y = n'_y$ (but not both). Note that this result is a special case of that in [Porter & Liboff, 2001b]. Even though the present problem has two *dov*, we note that there are additional requirements on the quantum numbers than those previously derived. The quantum numbers corresponding to movable-boundary variables have symmetry requirements that must be met so that the cross terms one obtains by taking the expectation of the Schrödinger equation do not vanish. Porter and Liboff [2001b] proved that there are symmetry requirements for quantum numbers corresponding to fixed-boundary

variables, but the conditions they found are not sufficient ones for the two *dov* rectangular quantum billiard. Indeed, we have just shown that this billiard has stronger requirements than those previously derived. It is not currently known whether this is true for all two *dov* billiards or whether the symmetry requirements are more stringent specifically for the present configuration.

4.1. Case One: Absence of Coupling Between States

Let us now examine the case without cross terms. That is, μ_{jk} vanishes for all $j, k \in \{1, 2\}$. We will show in the present section the conditions under which this case leads to chaotic behavior. Taking the expectation of the Schrödinger equation (13), one obtains the equations of motion:

$$i\dot{A}_j = \frac{1}{\hbar} \left(\frac{\varepsilon_a^{(j)}}{a^2} + \frac{\varepsilon_b^{(j)}}{b^2} \right), \quad j \in \{1, 2\}. \tag{22}$$

Integrating these equations for $j \in \{1, 2\}$ gives

$$A_j = C_j \exp \left[-\frac{i}{\hbar} \int \left(\frac{\varepsilon_a^{(j)}}{a^2} + \frac{\varepsilon_b^{(j)}}{b^2} \right) dt \right], \tag{23}$$

where C_j is a constant of integration. Since A_j 's only time-dependence is a phase factor, it follows that $|A_j|^2 = |C_j|^2$ is a constant. Recall that the evolution of the present system is determined by the Hamiltonian

$$\begin{aligned} H(a, P_a, b, P_b) &\equiv \frac{P_a^2}{2M_a} + \frac{P_b^2}{2M_b} + K(A_1, A_2, a, b) \\ &\quad + V(a, b), \end{aligned} \tag{24}$$

where the kinetic energy $K(A_1, A_2, a, b)$ is separable in the sense that

$$K(A_1, A_2, a, b) = K_1(A_1, A_2, a) + K_2(A_1, A_2, b) \tag{25}$$

and is given by

$$\begin{aligned} K &= \left(\frac{\varepsilon_a^{(1)}}{a^2} + \frac{\varepsilon_b^{(1)}}{b^2} \right) |A_1|^2 + \left(\frac{\varepsilon_a^{(2)}}{a^2} + \frac{\varepsilon_b^{(2)}}{b^2} \right) |A_2|^2 \\ &= \frac{\varepsilon_a^{(1)} |C_1|^2 + \varepsilon_a^{(2)} |C_2|^2}{a^2} + \frac{\varepsilon_b^{(1)} |C_1|^2 + \varepsilon_b^{(2)} |C_2|^2}{b^2}. \end{aligned} \tag{26}$$

The evolution of this Hamiltonian system is described by

$$\begin{aligned} \dot{a} &= \frac{P_a}{M_a} \\ \dot{P}_a &= -\frac{\partial V}{\partial a} + \frac{2}{a^3}(\varepsilon_a^{(1)}|C_1|^2 + \varepsilon_a^{(2)}|C_2|^2) \\ \dot{b} &= \frac{P_b}{M_b} \\ \dot{P}_b &= -\frac{\partial V}{\partial b} + \frac{2}{b^3}(\varepsilon_b^{(1)}|C_1|^2 + \varepsilon_b^{(2)}|C_2|^2). \end{aligned} \tag{27}$$

Stationary points (27) satisfy $P_a = P_b = 0$,

$$\frac{\partial V}{\partial a} = \frac{2}{a^3}(\varepsilon_a^{(1)}|C_1|^2 + \varepsilon_a^{(2)}|C_2|^2), \tag{28}$$

and

$$\frac{\partial V}{\partial b} = \frac{2}{b^3}(\varepsilon_b^{(1)}|C_1|^2 + \varepsilon_b^{(2)}|C_2|^2). \tag{29}$$

Defining

$$\eta_a \equiv \varepsilon_a^{(1)}|C_1|^2 + \varepsilon_a^{(2)}|C_2|^2, \tag{30}$$

$$\eta_b \equiv \varepsilon_b^{(1)}|C_1|^2 + \varepsilon_b^{(2)}|C_2|^2, \tag{30'}$$

one finds that, for any equilibrium point of (27), if

$$\begin{aligned} \frac{\partial^2 V}{\partial a^2} \frac{\partial^2 V}{\partial b^2} - \left(\frac{\partial^2 V}{\partial a \partial b} \right)^2 + \frac{6\eta_a}{a^4} \frac{\partial^2 V}{\partial b^2} \\ + \frac{6\eta_b}{b^4} \frac{\partial^2 V}{\partial a^2} + \frac{36\eta_a \eta_b}{a^4 b^4} \geq 0, \end{aligned} \tag{31}$$

then every eigenvalue corresponding to that equilibrium point has zero real part, so it is elliptic (and hence linearly stable). (Equilibrium points are defined to be elliptic when the real part of all of their associated eigenvalues is zero.) In particular, if the potential has a single minimum, then every equilibrium point is elliptic. Note that the curve on which equality holds in (31) is a bifurcation curve, as the topology of the equilibria changes with the sign of the expression. Recall that $V(a, b)$ is a known function so that the left-hand side of (31) is also known.

The above analysis also holds if one considers only a single state. In other words, in a two *dof* quantum billiard in an inseparable potential, one obtains a system that exhibits chaotic behavior even if one considers only one state. (The equations are of the same form as those above, since there is no coupling in the present case.) For one *dof* quantum

billiards, a two-term superposition state is required for chaos to occur [Liboff & Porter, 2000; Porter & Liboff, 2001b]. We may state this result as the following theorem.

Theorem 2. *Consider a quantum billiard with more than one *dof* in an inseparable potential. Any superposition state — even one with a single wavefunction — will exhibit chaotic behavior in some region of parameter space.*

If, however, the potential V is separable in the sense that

$$V(a, b) = V_1(a) + V_2(b), \tag{32}$$

then the Hamiltonian $H(a, P_a, b, P_b)$ is separable in the same sense. That is,

$$H(a, P_a, b, P_b) = H_1(a, P_a) + H_2(b, P_b), \tag{33}$$

and this decoupling of the two degree-of-freedom (*dof*) into two one *dof* Hamiltonians corresponds to a decoupling of the present four-dimensional autonomous evolution equations into a pair of two-dimensional autonomous dynamical systems, whose nonchaotic properties are known [Guckenheimer & Holmes, 1983; Wiggins, 1990; Strogatz, 1994]. The fact that the present quantum billiard is nonchaotic if there are no cross terms and a separable potential also follows from the discussion in [Porter & Liboff, 2001b], in which the following theorem was proved:

Theorem 3. *Consider a quantum billiard on a Riemannian manifold with *s dof* satisfying a couple of technical, geometric conditions. If all the cross terms μ_{jk} of a superposition state vanish and the Hamiltonian is separable, then there is a decoupling into a set of two-dimensional autonomous dynamical systems, which implies that the superposition state is nonchaotic.*

If the potential is inseparable, however, one can obtain chaotic behavior even if the cross term μ_{jk} vanishes. Consider, for example, the anharmonic potential

$$\begin{aligned} V(a, b) &= \frac{V_a}{a_0^2}(a - a_0)^2 + \frac{V_b}{b_0^2}(b - b_0)^2 \\ &+ \frac{V_0}{a_0 b_0}(a - a_0)(b - b_0). \end{aligned} \tag{34}$$

In this case,

$$\frac{\partial^2 V}{\partial a^2} = \frac{2V_a}{a_0^2}, \quad \frac{\partial^2 V}{\partial b^2} = \frac{2V_b}{b_0^2}, \quad \frac{\partial^2 V}{\partial a \partial b} = \frac{V_0}{a_0 b_0}, \quad (35)$$

so an equilibrium point of (27) is elliptic if and only if

$$\begin{aligned} \frac{4V_a V_b}{a_0^2 b_0^2} - \frac{V_0^2}{a_0^2 b_0^2} + \frac{12\eta_a V_b}{a^4 b_0^2} + \frac{12\eta_b V_a}{a_0^2 b^4} \\ + \frac{36\eta_a \eta_b}{a^4 b^4} \geq 0. \end{aligned} \quad (36)$$

In (36), a and b refer to equilibrium values. Note that the present system of Eq. (27) has a bifurcation curve when equality holds in the above equation.

Figures 1–6 show various Poincaré maps for the superposition state

$$\begin{aligned} \psi = \alpha A_1 \cos\left(\frac{\pi x}{a}\right) \cos\left(\frac{3\pi y}{b}\right) \\ + \alpha A_2 \sin\left(\frac{2\pi x}{a}\right) \sin\left(\frac{4\pi y}{b}\right). \end{aligned} \quad (37)$$

Each figure has the parameter values $\hbar = 1$, $m = 1$, $\varepsilon_a^{(1)} = \hbar^2 \pi^2 / 2m \approx 4.93480220054$, $\varepsilon_b^{(1)} = 9\hbar^2 \pi^2 / 2m \approx 44.4132198049$, $\varepsilon_a^{(2)} = 4\hbar^2 \pi^2 / 2m \approx 19.7392088022$, $\varepsilon_b^{(2)} = 15\hbar^2 \pi^2 / 2m \approx 78.9568352087$, $a_0 = 1.25$, $b_0 = 0.75$, $|C_1|^2 = 4$, $|C_2|^2 = 8$, $M_a = 10$ and $M_b = 5$. Figure 1 shows the Poincaré map corresponding to the cut $P_a = 0$ in the (b, P_b) -plane for the parameter values $V_0/(a_0 b_0) = 5$, $V_a/(a_0^2) = 10$ and $V_b/(b_0^2) = 2$. Figure 2 shows the corresponding projection in the (a, b) -plane. Figures 3–6 have the parameter values $V_0/(a_0 b_0) = 12$, $V_a/(a_0^2) = 1$ and $V_b/(b_0^2) = 3$. Figures 3 and 5 depict Poincaré maps for $P_a = 0$ for different initial conditions in the (b, P_b) -plane. Figures 4 and 6 correspond respectively to Figs. 3 and 5 and show projections of the Poincaré maps in the (a, b) -plane. Note that the plots are of the same form for any constant $c > 0$, $|C_1|^2 + |C_2|^2 = |A_1|^2 + |A_2|^2 = c$, so where only the relative sizes of $|C_1|^2$ and $|C_2|^2$ are relevant.

We note that the chaotic behavior in the variables (a, b, P_a, P_b) is classical Hamiltonian chaos, since the displacements and momenta of the boundaries are classical quantities. However, the quantum-mechanical wave $\psi(x, y, t; a(t), b(t))$ depends on the chaotic variables a and b . The individual normal modes (eigenfunctions) depend on these variables as well. The wavefunction ψ as

well as the normal modes are hence examples of so-called quantum-mechanical wave chaos [Blümel & Reinhardt, 1997]. (The wave ψ is a linear combination of chaotic normal modes.) This is one of the signatures of quantum chaos. We note, however, that it is important to contrast this with chaos that one obtains in the coupled classical and quantum systems that occurs when there is coupling between two or more superposition states. In this case, one observes chaotic quantum waves resulting from a classical system that is chaotic by itself. Previously, Porter and Liboff [Liboff & Porter, 2000; Porter & Liboff, 2001a; Porter & Liboff, 2001b] and Blümel and Esser [1994] observed chaotic classical and quantum subsystems that were integrable if considered separately. (In one *dov* quantum billiards, the Hamiltonian has a single classical degree-of-freedom due to the motion of the boundary.) The distinction, then, is that in the present case (without coupling), the classical Hamiltonian chaos drives the quantum-mechanical wave chaos, whereas previously, the quantum-mechanical wave chaos was due to coupling between classical and quantum systems. (That is, we examined the coupling between the billiard’s boundary and the particle bouncing around inside it.)

4.2. Case Two: Presence of Coupling Between States

We now examine an example of a two-term superposition with nonvanishing cross terms. We showed earlier that in a two-term superposition

$$|\psi\rangle = \psi_1 |n_x n_y\rangle + \psi_2 |n'_x n'_y\rangle, \quad (38)$$

one must have either $n_x = n'_x$ or $n_y = n'_y$ in order to obtain nonzero coupling coefficients. Without loss of generality, consider the case in which $n_y = n'_y$. The evolution equations for $n_x = n'_x$ are obtained by reversing the roles of the variables (a, P_a) and (b, P_b) . Taking expectations and equating coefficients gives

$$i\dot{A}_n = \sum_{j=1}^2 D_{nj} A_j, \quad (39)$$

where

$$(D_{nj}) = \begin{pmatrix} \frac{1}{\hbar} \left(\frac{\varepsilon_a^{(1)}}{a^2} + \frac{\varepsilon_b^{(1)}}{b^2} \right) & -i\mu_{nq} \frac{\dot{a}}{a} \\ i\mu_{nq} \frac{\dot{a}}{a} & \frac{1}{\hbar} \left(\frac{\varepsilon_a^{(2)}}{a^2} + \frac{\varepsilon_b^{(2)}}{b^2} \right) \end{pmatrix} \quad (40)$$

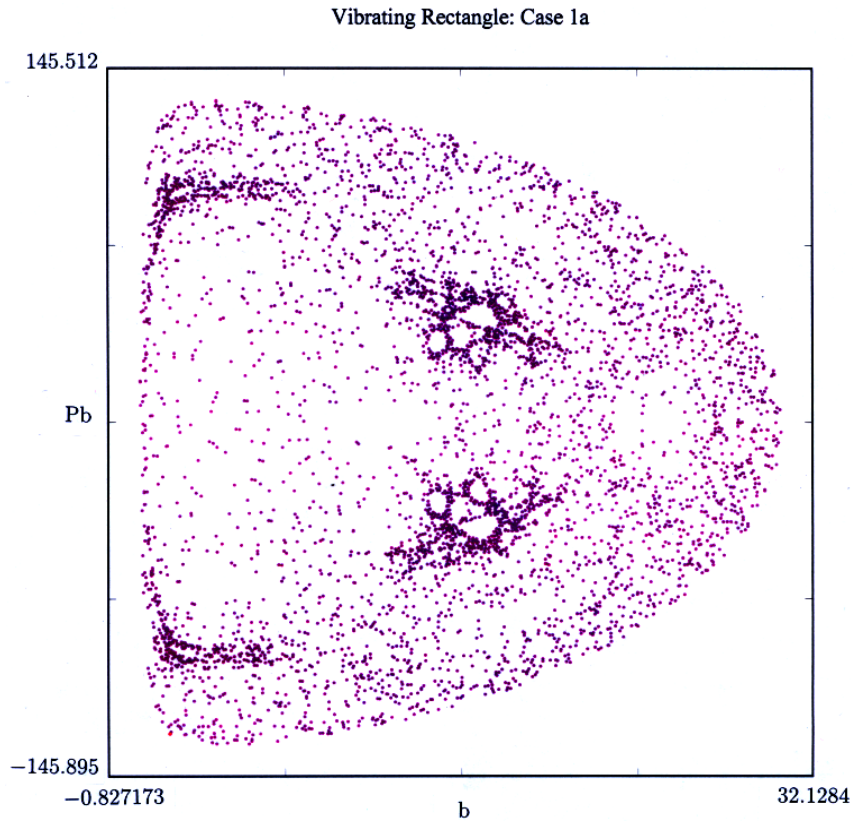


Fig. 1. Poincaré section for the cut $P_a = 0$ in the (b, P_b) -plane with potential parameters $V_0 = 5$, $V_a = 10$ and $V_b = 2$.

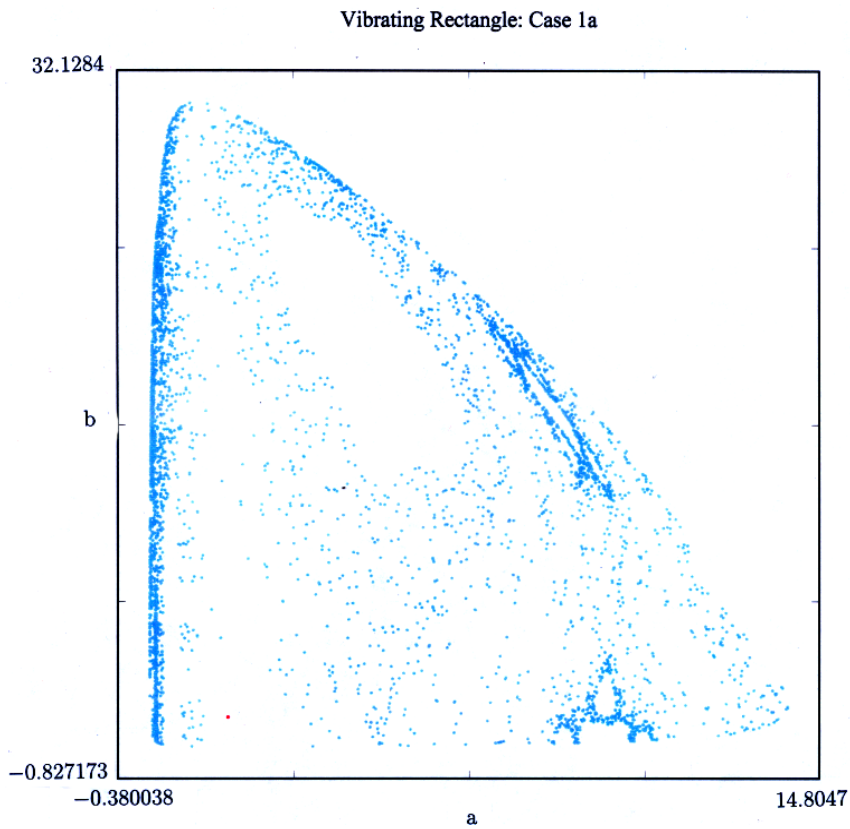


Fig. 2. Poincaré section for the cut $P_a = 0$ in the (a, b) -plane with potential parameters $V_0 = 5$, $V_a = 10$ and $V_b = 2$.

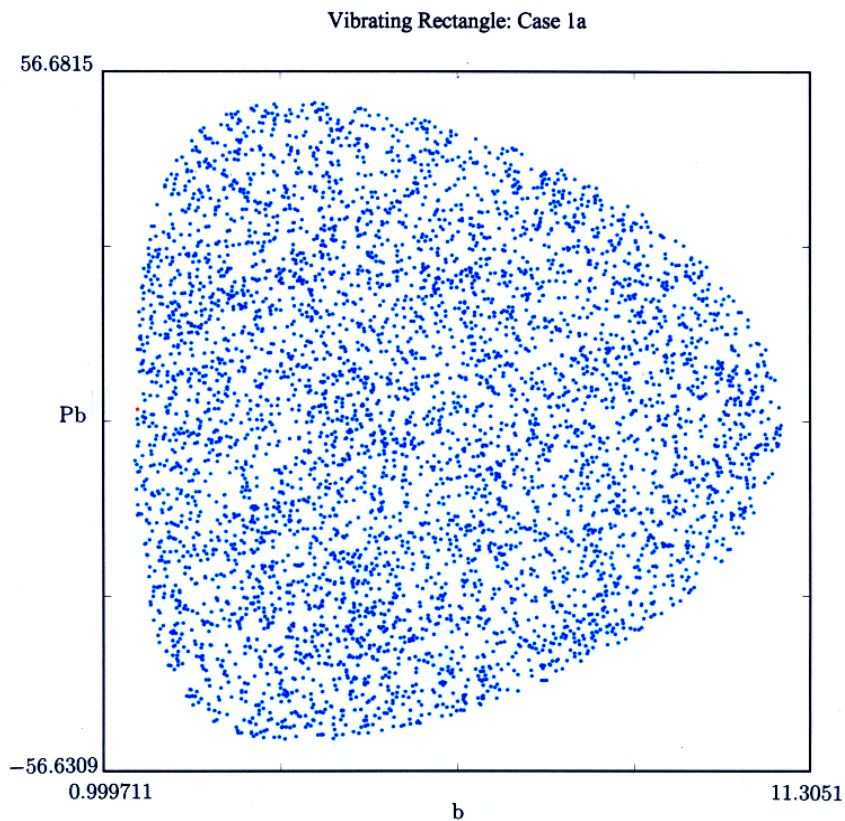


Fig. 3. Poincaré section for the cut $P_a = 0$ in the (b, P_b) -plane with potential parameters $V_0 = 12$, $V_a = 1$ and $V_b = 3$.

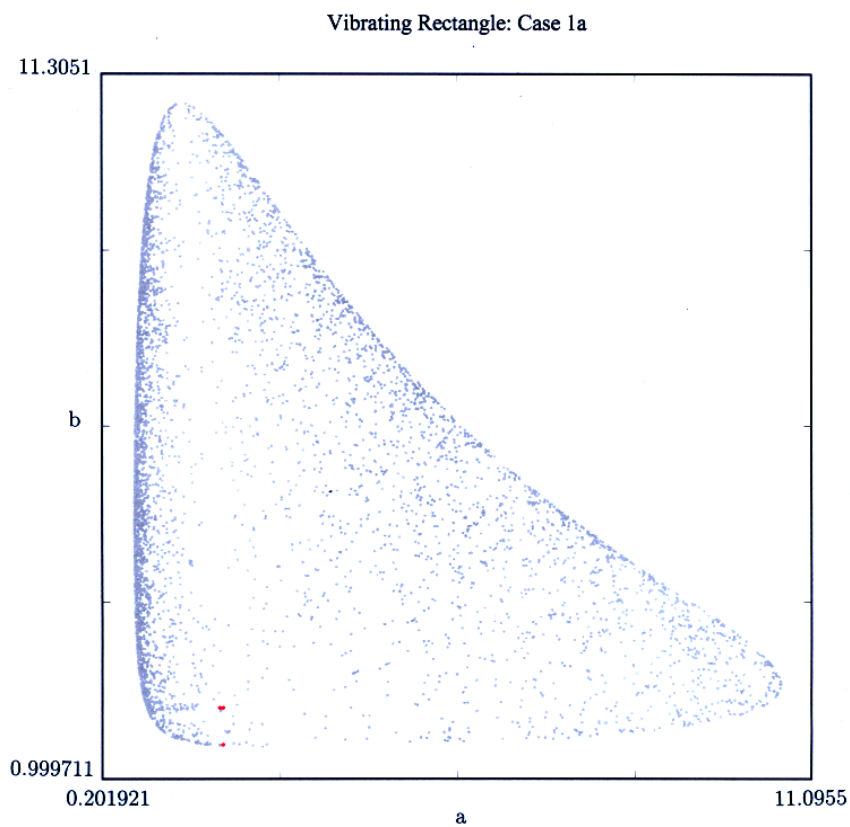


Fig. 4. Poincaré section for the cut $P_a = 0$ in the (a, b) -plane with potential parameters $V_0 = 12$, $V_a = 1$ and $V_b = 3$.

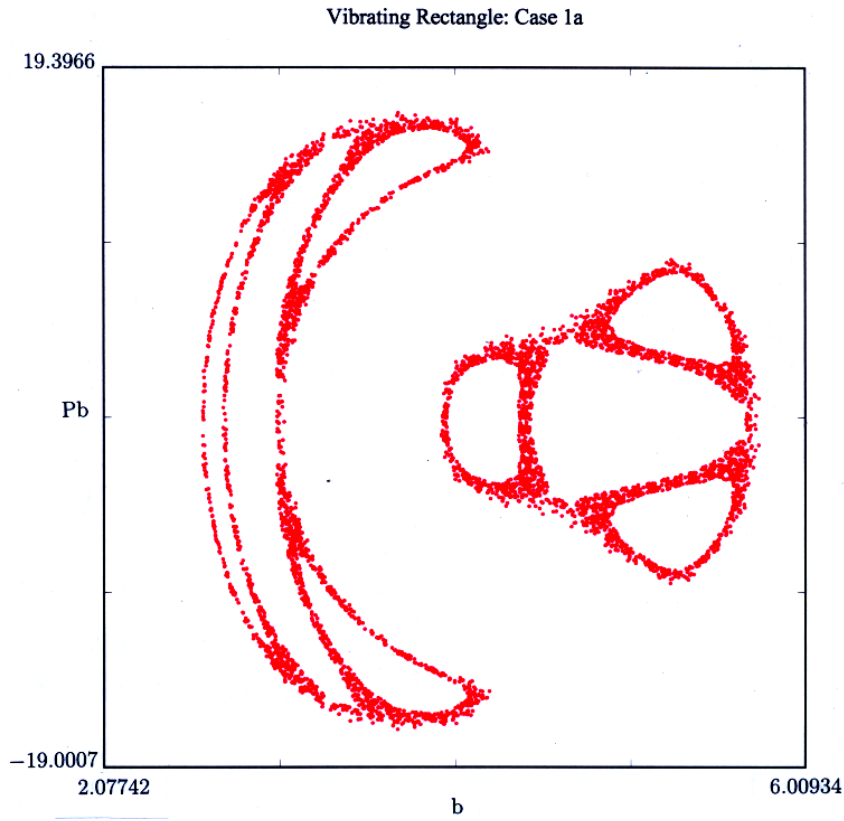


Fig. 5. Poincaré section for the cut $P_a = 0$ in the (b, P_b) -plane with potential parameters $V_0 = 12$, $V_a = 1$ and $V_b = 3$.

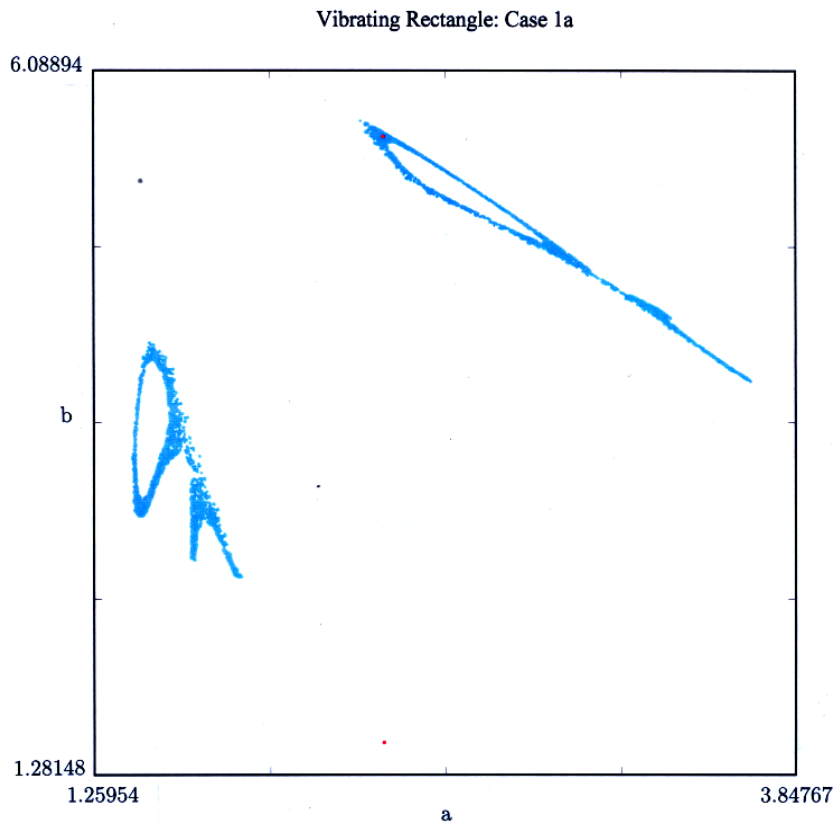


Fig. 6. Poincaré section for the cut $P_a = 0$ in the (a, b) -plane with potential parameters $V_0 = 12$, $V_a = 1$ and $V_b = 3$.

and μ_{nq} is the coefficient of $A_n A_q^*$. Defining the density matrix [Liboff, 1998] $\rho_{mn} \equiv A_m A_n^*$ and transforming to Bloch variables [Allen & Eberly, 1987]

$$x = \rho_{12} + \rho_{21}, y = i(\rho_{21} - \rho_{12}), z = \rho_{22} - \rho_{11} \tag{41}$$

and noting that $\varepsilon_b^{(1)} = \varepsilon_b^{(2)}$ gives the following equations:

$$\dot{x} = -\frac{\omega_0^{(a)} y}{a^2} - \frac{2\mu_{nq} P_a z}{M_a a}, \tag{42a}$$

$$\dot{y} = \frac{\omega_0^{(a)} x}{a^2}, \tag{42b}$$

$$\dot{z} = \frac{2\mu_{nq} P x}{M_a a}. \tag{42c}$$

In these equations,

$$\omega_0^{(a)} \equiv \frac{\varepsilon_a^{(2)} - \varepsilon_a^{(1)}}{\hbar}. \tag{43}$$

Note that the above equations depend only on the dimension a and not on b . When taking expectations, this follows from the fact that $n_y = n'_y$. Recall that with the complementary condition $n_x = n'_x$, the roles of the displacements $a(t)$ and $b(t)$ are reversed.

Using Bloch variables (41), one computes

$$K(A_1, A_2, a, b) = \frac{(\varepsilon_a^+ + z\varepsilon_a^-)}{a^2} + \frac{\varepsilon_b^+}{b^2} \tag{44}$$

where

$$\varepsilon_a^\pm \equiv \frac{\varepsilon_a^{(2)} \pm \varepsilon_a^{(1)}}{2} \tag{45}$$

and

$$\varepsilon_b^\pm \equiv \frac{\varepsilon_b^{(2)} \pm \varepsilon_b^{(1)}}{2}. \tag{46}$$

Note that because $\varepsilon_b^{(1)} = \varepsilon_b^{(2)}$, ε_b^- vanishes for the present superposition state. In a two-term superposition for which $n_x = n'_x$, the parameter $\varepsilon_a^- = 0$.

The present superposition state has a Hamiltonian given by

$$H(a, P_a, b, P_b) = \frac{P_a^2}{2M_a} + \frac{P_b^2}{2M_b} + K(z, a, b) + V(a, b). \tag{47}$$

This leads to Hamilton's equations

$$\begin{aligned} \dot{a} &= \frac{\partial H}{\partial P_a}, \\ \dot{P}_a &= -\frac{\partial H}{\partial a}, \\ \dot{b} &= \frac{\partial H}{\partial P_b}, \\ \dot{P}_b &= -\frac{\partial H}{\partial b}. \end{aligned} \tag{48}$$

We thus find that

$$\dot{a} = \frac{P_a}{M_a} \tag{49}$$

and

$$\dot{b} = \frac{P_b}{M_b}. \tag{49'}$$

One also finds that

$$\begin{aligned} \dot{P}_a &\equiv -\frac{\partial V}{\partial a} - \frac{\partial K}{\partial a} \\ &= -\frac{\partial V}{\partial a} + \frac{2}{a^3}[\varepsilon_a^+ + \varepsilon_a^-(z - \mu_{nq}x)], \end{aligned} \tag{50}$$

and that

$$\dot{P}_b \equiv -\frac{\partial V}{\partial b} - \frac{\partial K}{\partial b} = -\frac{\partial V}{\partial b} + \frac{2\varepsilon_b^+}{b^3}. \tag{51}$$

Stationary points of the present vector field satisfy $P_a = P_b = x = y = 0$, $z = \pm 1$, $a = a_\pm$ and $b = b_\pm$, where a_\pm satisfies the equation $\dot{P}_a = 0$ for the $z = 1$ and $z = -1$, respectively, and b_\pm does the same with the equation $\dot{P}_b = 0$. That is, a_\pm satisfies

$$\frac{2}{a_\pm^3}(\varepsilon_a^+ \pm \varepsilon_a^-) = \frac{\partial V}{\partial a} \Big|_{a=a_\pm} \tag{52}$$

and b_\pm satisfies

$$\frac{2\varepsilon_b^+}{b_\pm^3} = \frac{\partial V}{\partial b} \Big|_{b=b_\pm}. \tag{53}$$

As in the case without cross terms, one can examine both separable potentials and inseparable potentials. In the former case, one observes a decoupling in the dynamical equations so that the evolution of (x, y, z, a, P_a) and that of (b, P_b) are completely independent of each other. In this situation, the analysis of (x, y, z, a, P_a) reduces to that for a one *dof* quantum billiard, although one can still obtain meaningful information by comparing a and P_a to b and P_b . In general, one can take the

point of view that (b, P_b) , whose dynamics are integrable when V is separable, produce useful insights when compared side-by-side with (a, P_a) , as demonstrated by Figs. (7)–(11). This point of view should prove illuminating for future research when considering the rectangular quantum billiard in which some motion (such as $a(t)$) is prescribed.

For numerical simulations, consider the superposition state

$$\psi = \alpha A_1(t) \cos\left(\frac{\pi x}{a(t)}\right) \cos\left(\frac{\pi y}{b(t)}\right) + \alpha A_2(t) \cos\left(\frac{3\pi x}{a(t)}\right) \cos\left(\frac{\pi y}{b(t)}\right). \quad (54)$$

In this case, $\mu_{12} = 3/4$. Recall once more that if $n_x = n'_x$ rather than $n_y = n'_y$, then the roles of (a, P_a) and (b, P_b) are reversed. This includes the results concerning decoupling in the present superposition state.

Consider first the harmonic potential

$$V(a, b) = \frac{V_a}{a_0^2}(a - a_0)^2 + \frac{V_b}{b_0^2}(b - b_0)^2, \quad (55)$$

which is separable. The (x, y, z, a, P_a) components of the equilibria are just as in the linear vibrating billiard. A simple calculation shows that all equilibria also satisfy

$$\frac{2\varepsilon_b^+}{b_{\pm}^3} = \frac{2V_b}{b_0^2}(b_{\pm} - b_0). \quad (56)$$

Poincaré maps for the harmonic potential are shown in Figs. 7–11. These depict, respectively, the cut $x = 0$ projected into the (a, b) -plane, the cut $x = 0$ in the (a, P_a) -plane, the cut $x = 0$ in the (b, P_b) -plane, the cut $x = 0$ in the (P_a, P_b) -plane, and the cut $P_a = 0$ in the (x, y) -plane. In units of $\hbar = 1$, we used the parameter values $m = 1$, $M_a = 10$, $\varepsilon_a^{(1)} = \hbar^2 \pi^2 / 2 \approx 4.9348022$, $\varepsilon_a^{(2)} = 9\hbar^2 \pi^2 / 2 \approx 44.4132198$, $\varepsilon_b^{(1)} = \varepsilon_b^{(2)} = \hbar^2 \pi^2 / 2$, $V_a/a_0^2 = 3$, $V_b/b_0^2 = 2$, $V_0/(a_0 b_0) = 0$ (since the potential is harmonic), $a_0 = 1.25$ and $b_0 = 1.75$ with the initial conditions $x(0) = \sin(0.95\pi) \approx 0.156434$, $y(0) = 0$, $z(0) = \cos(0.95\pi) \approx -0.987688$, $a(0) \approx 0.67880794$, $P_a(0) \approx -17.6821192$, $b(0) = 2$ and $P_b(0) = 3$.

Notice that Figs. 8 and 11 are very similar to chaotic Poincaré maps observed in one *dov* quantum billiards [Porter & Liboff, 2001b]. However,

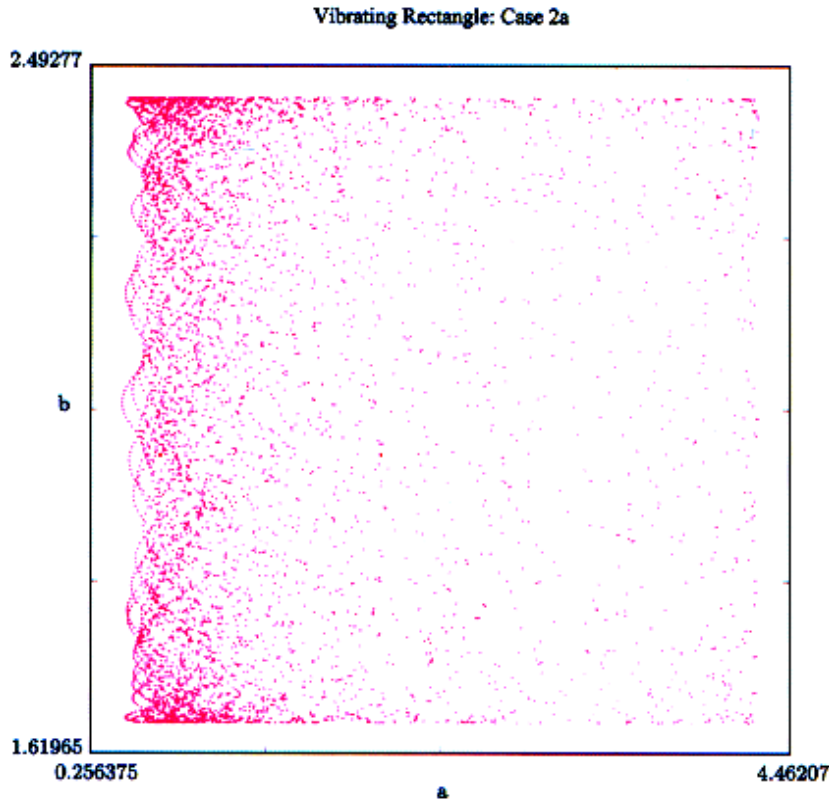


Fig. 7. Poincaré map for the harmonic potential with the cut $x = 0$ projected into the (a, b) -plane.

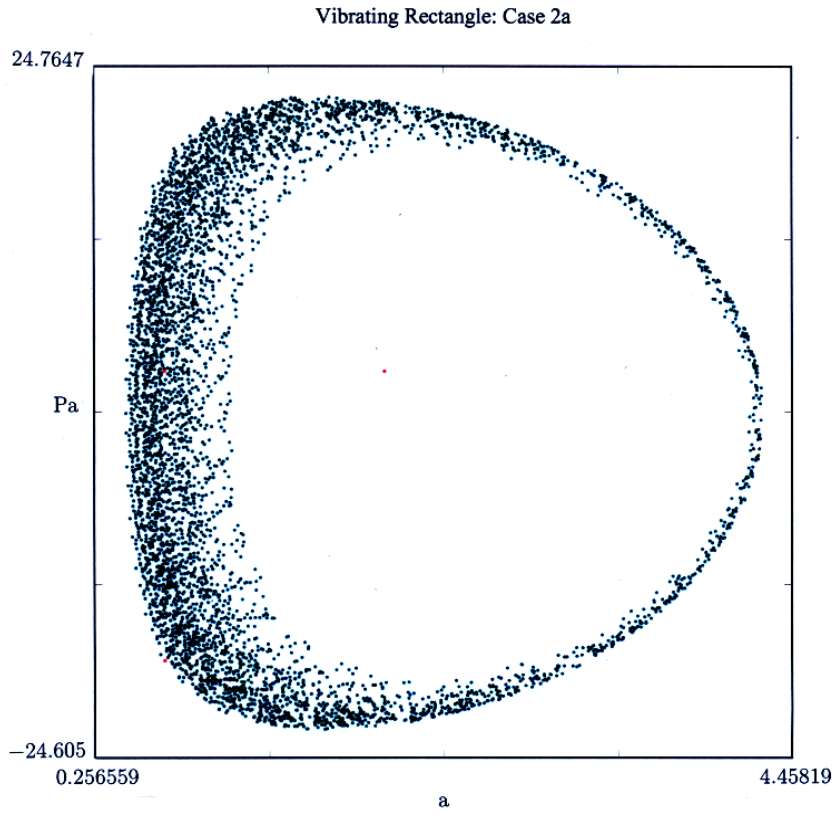


Fig. 8. Poincaré map for the harmonic potential with the cut $x = 0$ projected into the (a, P_a) -plane.

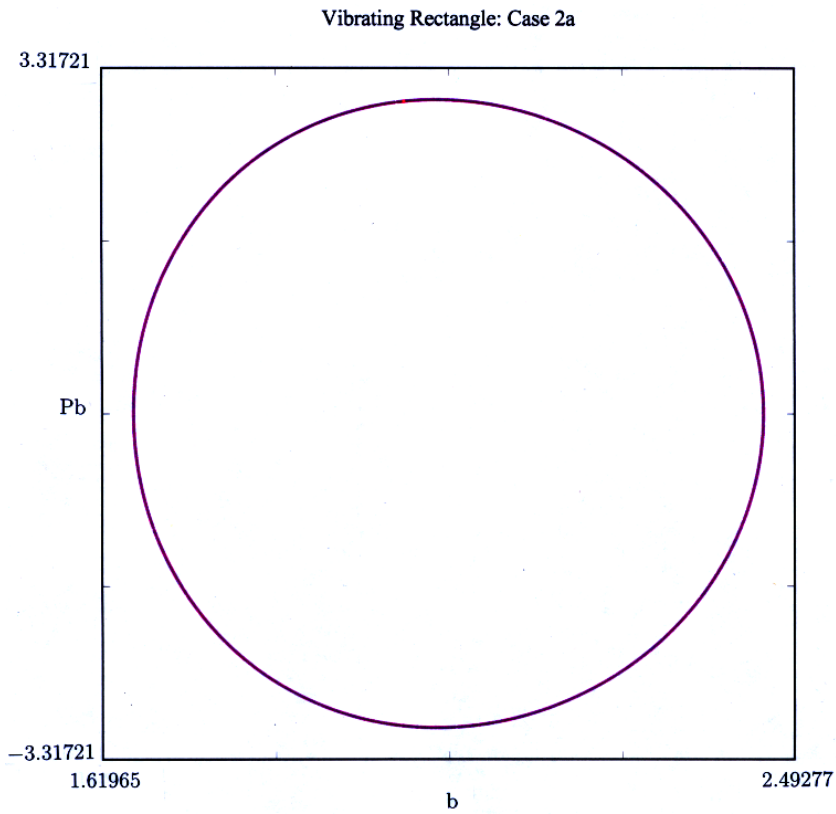


Fig. 9. Poincaré map for the harmonic potential with the cut $x = 0$ projected into the (b, P_b) -plane.

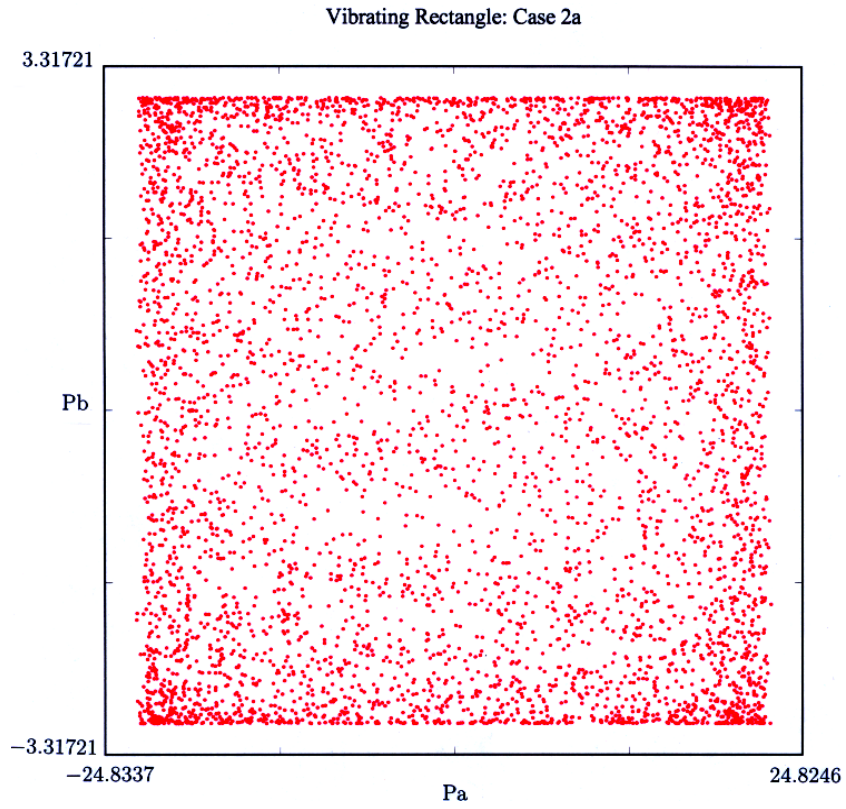


Fig. 10. Poincaré map for the harmonic potential with the cut $x = 0$ projected into the (P_a, P_b) -plane.

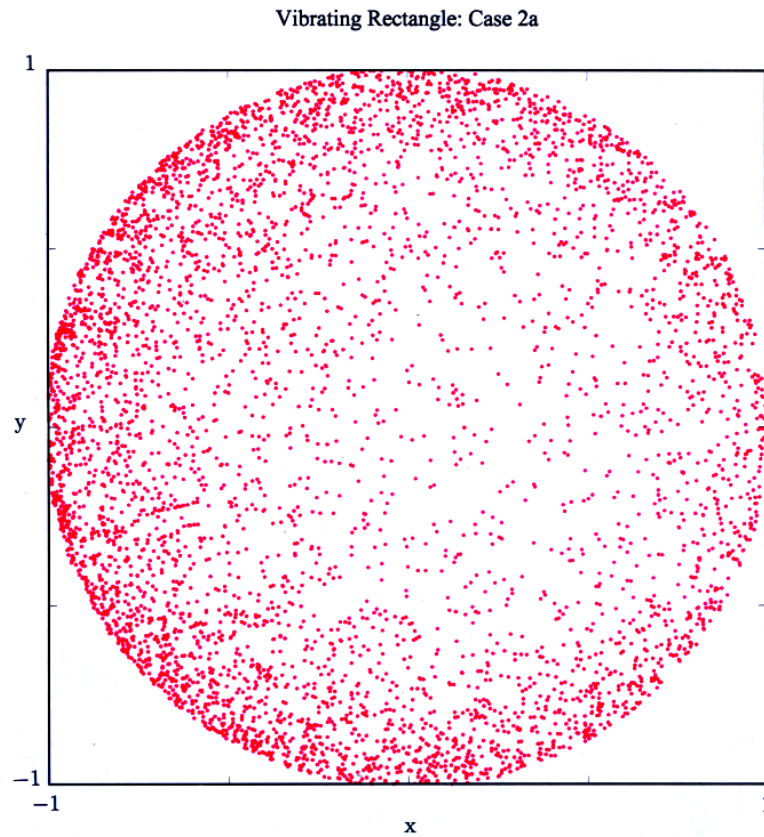


Fig. 11. Poincaré map for the harmonic potential with the cut $P_a = 0$ projected into the (x, y) -plane.

Fig. 9 shows that integrable motion is observed in the (b, P_b) -plane, as has to be the case in this decoupled situation. In contrast, the projection of the motion in the (a, P_a) -plane is simultaneously chaotic. This follows from the fact that the second term in the superposition state was excited only with respect to the length $a(t)$. We will discuss the behavior in Fig. 8 in detail shortly.

As another example, consider the anharmonic potential

$$V(a, b) = \frac{V_a}{a_0^2}(a - a_0)^2 + \frac{V_b}{b_0^2}(b - b_0)^2 + \frac{V_0}{a_0 b_0}(a - a_0)(b - b_0), \quad (57)$$

which is inseparable. Figures 12–19 depict, respectively, the cut $x = 0$ projected into the (a, b) -plane, the cut $x = 0$ in the (a, P_a) -plane, the cut $x = 0$ in the (b, P_b) -plane, the cut $x = 0$ in the (P_a, P_b) -plane, the cut $P_a = 0$ in the (b, P_b) -plane, the cut $P_a = 0$ in the (x, y) -plane, the cut $P_a = 0$ in the (x, z) -plane and the cut $P_a = 0$ in the (y, z) -plane. Each figure has the parameter values $\hbar = 1$, $m = 1$, $M_a = 10$, $\varepsilon_{a_1} = \hbar^2 \pi^2 / 2m \approx 4.93480220054$, $\varepsilon_{a_2} = 9\hbar^2 \pi^2 / 2m \approx 44.4132198049$, $\varepsilon_{b_1} = \varepsilon_{b_2} = \hbar^2 \pi^2 / 2m$, $\mu_{12} = 0.75$, $V_0 / (a_0 b_0) = 5$, $a_0 = 1.25$, $b_0 = 1.75$, $M_b = 10$, $V_a / (a_0^2) = 3$ and $V_b / (b_0^2) = 2$. Additionally, each plot has initial conditions $x(0) = \sin(0.95\pi) \approx 0.156434$, $y(0) = 0$ and $z(0) = \cos(0.95\pi) \approx -0.987688$, $a(0) \approx 1.57284768$, $P_a(0) \approx 1.920529801$, $b(0) = 2$, and $P_b(0) = 3$. Each plot except Fig. 14 exhibits chaotic behavior. (In general, the regions in parameter space in which the projection of the motion in the (b, P_b) -plane is integrable are larger than those in any other two-dimensional projection. For separable potentials such as the harmonic potential, moreover, the projection of the motion in this plane is always integrable because of the decoupling.)

We now contrast the behavior observed in a harmonic potential with that in an anharmonic one. The behavior of the two *dov* vibrating rectangular quantum billiard in the anharmonic potential is clearly distinguishable from that observed in single *dov* billiards. In both the (a, P_a) -plane and the (b, P_b) -plane, there are two distinct elliptical regions. Additionally — as expected — the behavior in the (b, P_b) -plane is more complicated than it was in the harmonic case, since one no longer has a decoupling in the evolution equations. In this particular plot, the behavior appears to be nonchaotic.

Note, however, that for the anharmonic potential, the Poincaré map *can* exhibit chaos in the (b, P_b) -plane and also that the double-ellipse structure is not present for all initial conditions. Therefore, one can distinguish plots from the vibrating rectangular billiard in the harmonic potential from those in an anharmonic potential. The present graphs are merely *one example* of behavioral differences. Also observe that the regions of space occupied in the configuration plane (a, b) as well as the momentum plane (P_a, P_b) are markedly more complicated for an anharmonic potential than they are for a harmonic one. This is due to the decoupling. In the present example, the two regions are simply connected in the harmonic case but not in the anharmonic one. Lastly, while the Bloch sphere in the harmonic case resembles those from one *dov* quantum billiards as it must, the Bloch sphere in the anharmonic case has much more structure in both chaotic and integrable situations.

Just as with one *dov* quantum billiards, one commonly obtains Poincaré maps that indicate that the billiard's boundary more often takes values corresponding to low $a(t)$ than high $a(t)$. Mathematically, this follows from the $1/a^2$ dependence of the particle's kinetic energy. Let us discuss the physical context of this behavior in some detail, in particular with reference to Fig. 8, which is similar to many plots from the radially vibrating spherical quantum billiard [Liboff & Porter, 2000; Porter & Liboff, 2001b, 2001a]. A low value of $a(t)$ leads to a larger kinetic energy, as the frequency of the particle's wavefunctions increases as a result of the smaller enclosure. The derivative of K with respect to a (which depends on $1/a^3$) becomes very large as well, and so $|\dot{P}_a|$ also becomes large. This often leads to a sign change in P_a and consequently a change in direction of the motion of that component of the wall. One thus often observes a large range of momenta P_a for small a . For large a , the potential $V(a, b)$ (as well as its derivative with respect to a) often becomes large and so one often observes a sign change in P_a around that point as well. (More complicated behavior can also occur, but this is the standard chaotic configuration that is depicted in Fig. 8.) The potential $V(a, b)$ is proportional to a^2 (and so its derivative with respect to a is proportional to a), whereas the derivative of the kinetic energy is proportional to $1/a^3$. Therefore, the range of momenta P_a is larger for small a than it is for large a . For a quartic potential

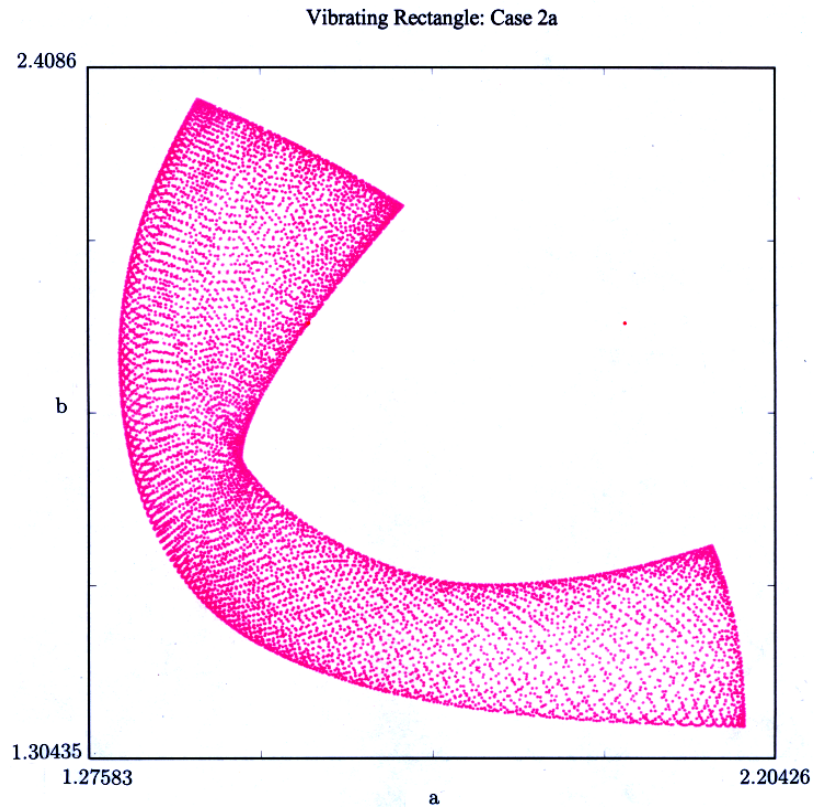


Fig. 12. Poincaré map for the anharmonic potential with the cut $x = 0$ projected into the (a, b) -plane.

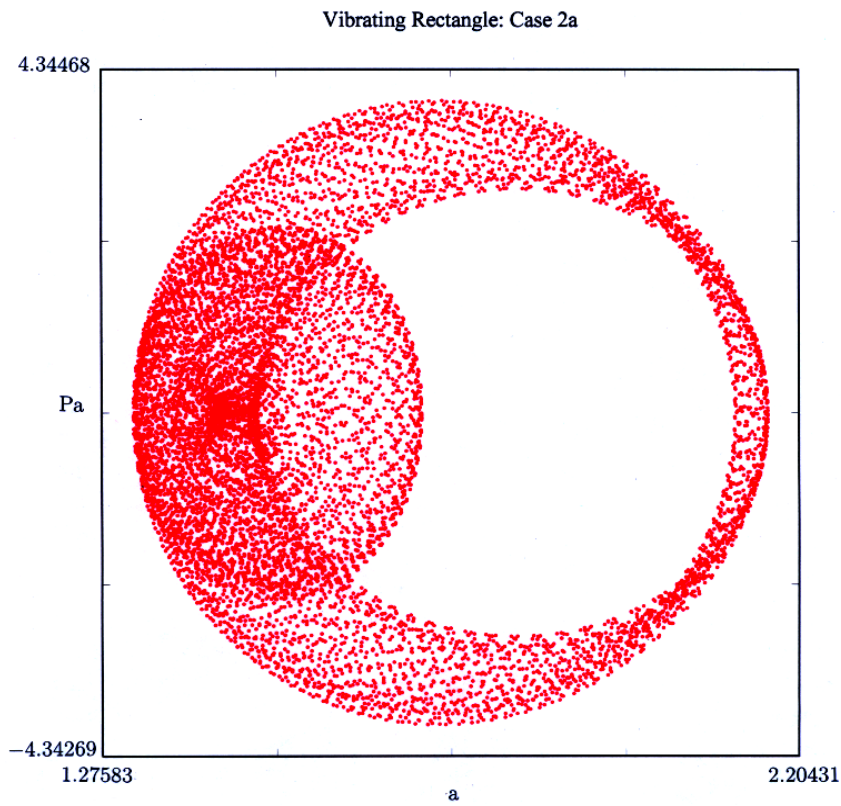


Fig. 13. Poincaré map for the anharmonic potential with the cut $x = 0$ projected into the (a, P_a) -plane.

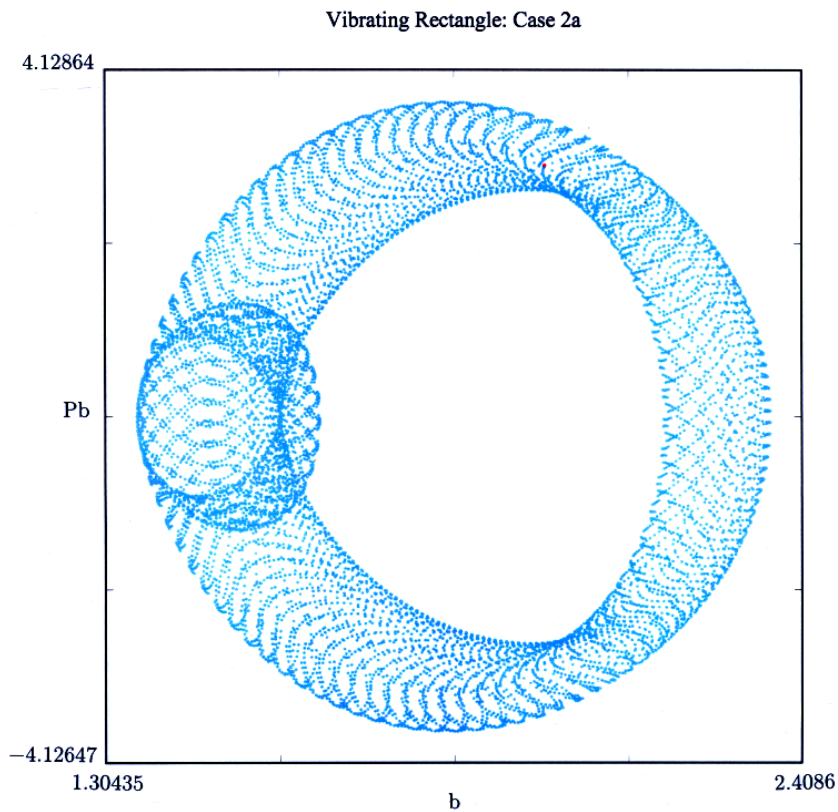


Fig. 14. Poincaré map for the anharmonic potential with the cut $x = 0$ projected into the (b, P_b) -plane.

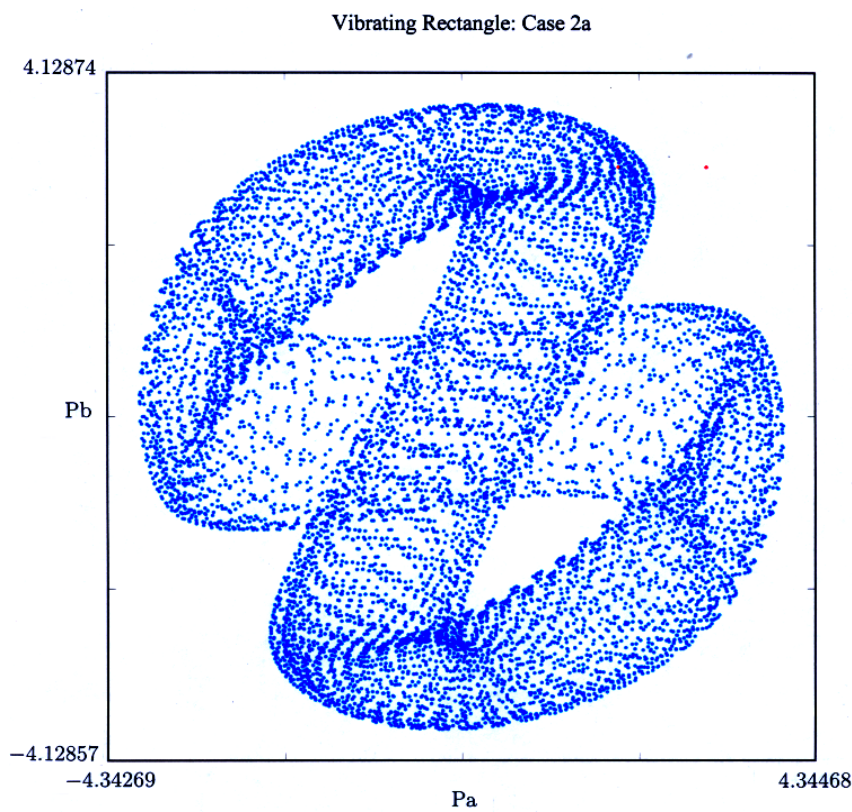


Fig. 15. Poincaré map for the anharmonic potential with the cut $x = 0$ projected into the (P_a, P_b) -plane.

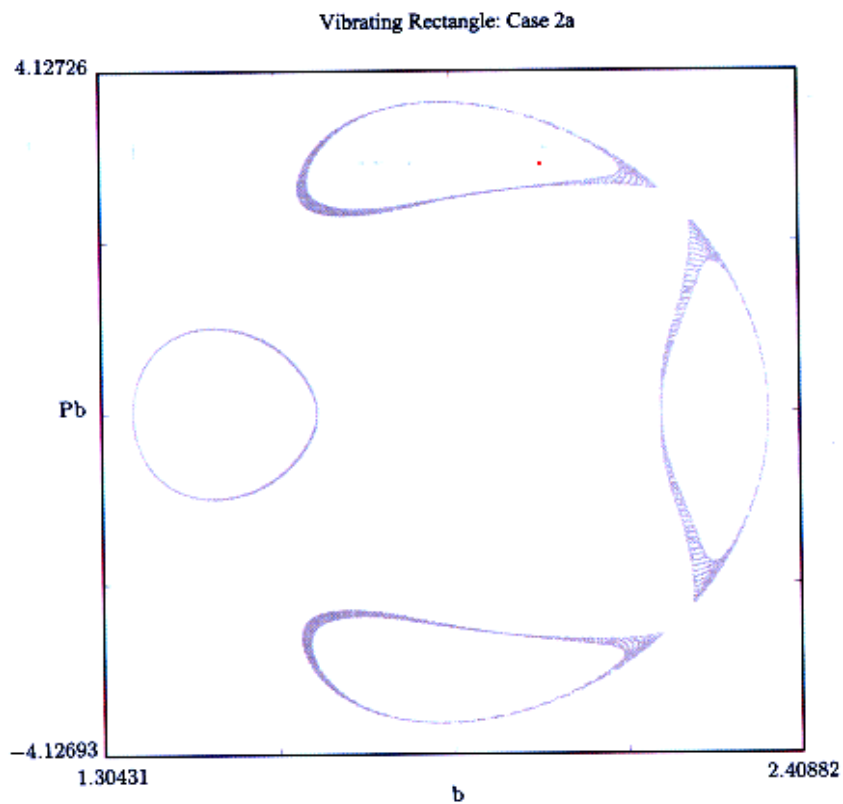


Fig. 16. Poincaré map for the anharmonic potential with the cut $P_a = 0$ projected into the (b, P_b) -plane.

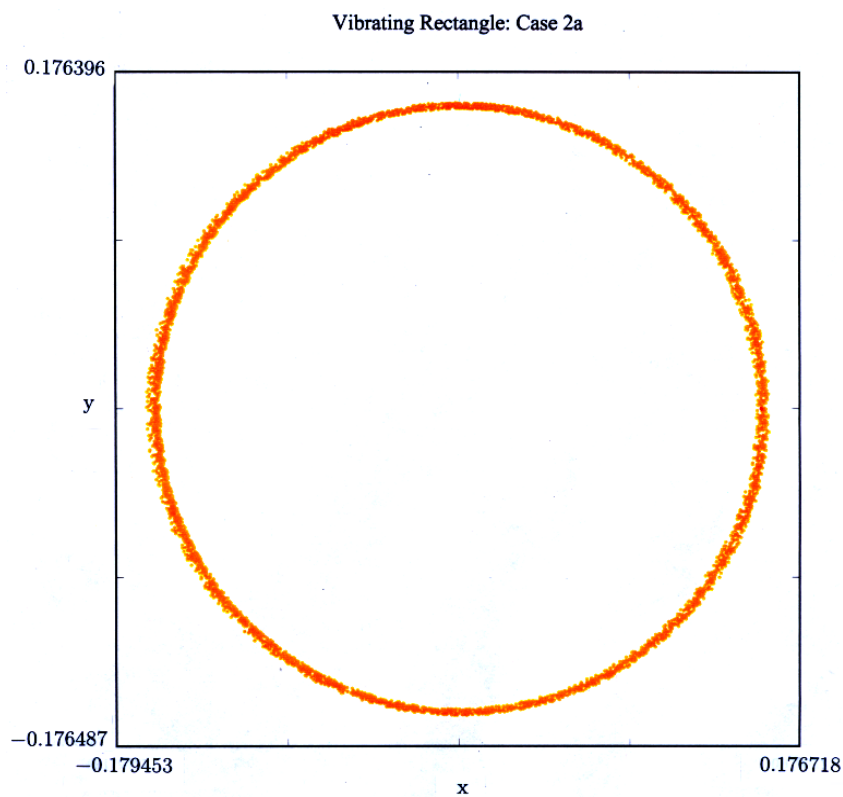


Fig. 17. Poincaré map for the anharmonic potential with the cut $P_a = 0$ projected into the (x, y) -plane.

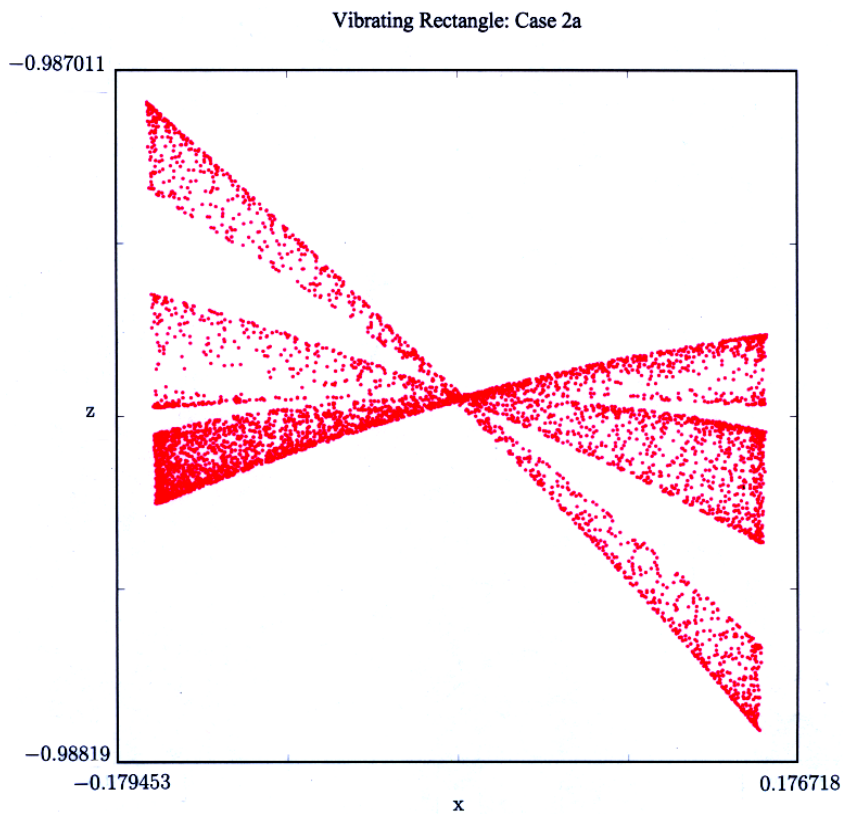


Fig. 18. Poincaré map for the anharmonic potential with the cut $P_a = 0$ projected into the (x, z) -plane.

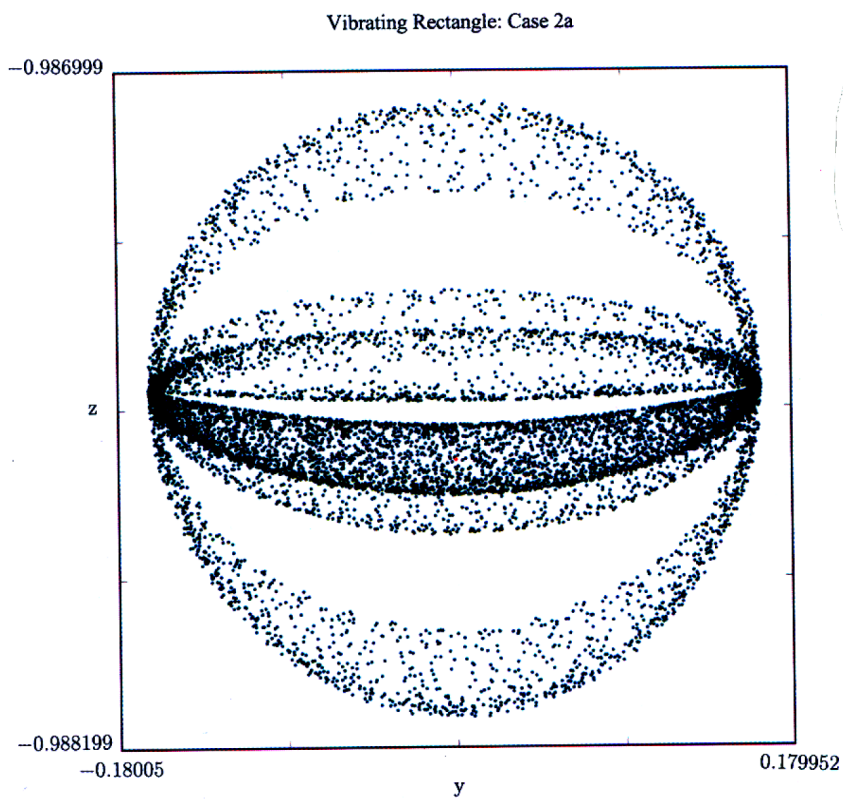


Fig. 19. Poincaré map for the anharmonic potential with the cut $P_a = 0$ projected into the (y, z) -plane.

Porter & Liboff, 2001a], one computes that

$$\frac{\partial V(a, b)}{\partial a} \propto a^3, \quad (58)$$

so the analogous configuration has an equally large range for P_a for both the upper and lower regimes of $a(t)$. In between a 's low and high regimes, the terms from the potential energy V and the kinetic energy K compete with each other, so $|\dot{P}_a|$ is not very large and the momentum P_a does not change signs. For small a , moreover, one often observes a higher density of points in the Poincaré map (for the cut $x = 0$). Indeed, the Bloch variable x often changes sign as a result of a change in sign of P_a , so such behavior is expected to occur for many initial conditions.

We note that the analytical methods that have been developed for vibrating quantum billiards correspond to applying the Born–Oppenheimer approximation [Blümel & Esser, 1994]. This approximation allows one to separate the time-dependence of the phase from that of the rest of the wave. In particular, this approximation reflects the fact that the eigenenergies of the vibrating quantum billiard are approximated as being equal to those of the associated stationary quantum billiard of the relevant geometry. The next term of the perturbative scheme (that we applied implicitly) includes the effect of so-called geometric phase (also known as Berry phase) [Zwanziger *et al.*, 1990]. The Born–Oppenheimer approximation corresponds to an adiabatic approximation. The quantity $K + V$ is the adiabatic potential of the (slow) classical variables a and b . The quantum variables (rerepresented by Bloch variables) are the fast variables in the present system. Blümel and Esser [1994] claim that the mixed quantum-classical system of vibrating quantum billiards is a caricature of diatomic molecules. In this interpretation, the preference for small values of a that is commonly observed corresponds to the preference for small inter-atomic distances in such dimers.

5. Comparison with One Degree-of-Vibration Quantum Billiards

It was shown previously that for an n -term superposition state of a one *dov* quantum billiard that at least one pair of the states must have the same fb quantum numbers in order for the superposition to exhibit quantum chaos [Porter & Liboff, 2001b].

Examination of the two *dov* rectangular quantum billiard in an anharmonic potential shows that one can observe quantum chaos without an analogous symmetry result in billiards with greater than one *dov* if the potential is inseparable. (The origin of this chaotic behavior, however, is the classical Hamiltonian chaos of the billiard's boundary rather than the coupling of classical (slow) and quantum-mechanical (fast) variables as is the case when two or more eigenstates are coupled.) If the potential is separable, we showed that an analogous symmetry requirement does hold. Moreover, even in the chaotic case, two *dov* billiards in separable potentials (as demonstrated by the harmonic potential) resemble the analogous single *dov* case because of the decoupling induced by the potential's separability. When one examines inseparable potentials (such as the anharmonic potential), one observes more complicated behavior.

6. Two Degrees-of-Vibration in n -Dimensional Rectangular Parallelepiped Quantum Billiards

One may generalize Theorem 1 to the case of a two *dov* n -dimensional rectangular parallelepiped quantum billiard. That is, $n - 2$ of the boundary dimensions are constant, but the other two vary in time. The case $n = 2$ is simply the rectangular quantum billiard with time-dependent length and width. This result follows almost immediately from Theorem 1. One does $n - 2$ integrations corresponding to the fb quantum numbers (which are the quantum numbers corresponding to time-invariant boundary variables), which gives unity by normalization considerations. This gives the same integral as in the previous case, and so the result follows by applying Theorem 1. We state Theorem 4 as follows:

Theorem 4. *Consider the n -dimensional rectangular parallelepiped quantum billiard with two *dov*. Consider a superposition of two eigenstates. The cross-term coefficients μ_{jk} and μ_{kj} ($j \neq k$) vanish if and only if one of the pair of mb -quantum numbers is symmetric. In other words, these coupling coefficients are nonzero if and only if either $n_x = n'_x$ or $n_y = n'_y$, where we assume without loss of generality that the time-dependent dimensions ($a_x(t)$, $a_y(t$)) of the billiard's boundary are those along the \hat{x} and \hat{y} axes. The coefficients μ_{jj} and μ_{kk} always vanish,*

and the relation $\mu_{jk} = -\mu_{kj}$ always holds. Moreover, μ_{jk} acts as a proportionality constant in front of a term of the form \dot{a}_x/a_x if $n_y = n'_y$ and \dot{a}_y/a_y if $n_x = n'_x$, and it is exactly as in the one-dimensional vibrating quantum billiard [Blümel & Esser, 1994; Blümel & Reinhardt, 1997]:

$$\mu_{jk} \equiv \mu_{nn'} = \frac{2nn'}{(n' + n)(n' - n)}. \quad (59)$$

In considering a superposition of more than two states, this theorem applies pairwise. (That is, there must exist some pair of states among those being superposed such that the above condition holds.)

7. Conclusion

In the present paper, we considered vibrations with two degrees-of-freedom in rectangular quantum billiards. We analyzed several superposition states and discussed the effects of symmetry on the equations of motion. (We stated and proved several theorems concerning these results.) We generalized this discussion to n -dimensional rectangular parallelepipeds with two degrees-of-vibration. We produced several sets of Poincaré sections, and we divided the analysis into four cases corresponding to the presence or absence of coupling terms and the choice of the harmonic or anharmonic potential. The behavior of the two *dov* rectangular quantum billiard in the harmonic potential was similar to the behavior of single *dov* systems, while its behavior in the anharmonic potential was considerably more complicated.

Acknowledgments

The authors would like to thank Sir Michael Berry, John Guckenheimer, Adrian Mariano, Eric Phipps and Richard Rand for fruitful discussions concerning the topic of this paper.

References

- Allen, L. & Eberly, J. H. [1987] *Optical Resonance and Two-Level Atoms* (Dover Publications, Inc., NY).
- Blümel, R. & Esser, B. [1994] "Quantum chaos in the Born–Oppenheimer approximation," *Phys. Rev. Lett.* **72**(23), 3658–3661.
- Blümel, R. & Reinhardt, W. P. [1997] *Chaos in Atomic Physics* (Cambridge University Press, Cambridge, England).
- Guckenheimer, J. & Holmes, P. [1983] *Nonlinear Oscillations, Dynamical Systems, and Bifurcations of Vector Field*, Applied Mathematical Sciences, Vol. 42 (Springer-Verlag, NY).
- Gutzwiller, M. C. [1990] *Chaos in Classical and Quantum Mechanics*, Interdisciplinary Applied Mathematics, Vol. 1 (Springer-Verlag, NY).
- Johnson, C. [1987] *Numerical Solution of Partial Differential Equations by the Finite Element Method* (Cambridge University Press, Cambridge, England).
- Liboff, R. L. [1998] *Introductory Quantum Mechanics*, 3rd edition (Addison-Wesley, San Francisco, CA).
- Liboff, R. L. & Porter, M. A. [2000] "Quantum chaos for the radially vibrating spherical billiard," *Chaos* **10**(2), 366–370.
- Porter, M. A. & Liboff, R. L. [2001a] "Bifurcations in one degree-of-vibration quantum billiards," *Int. J. Bifurcation and Chaos* **11**(4), 903–911.
- Porter, M. A. & Liboff, R. L. [2001b] "Vibrating quantum billiards on Riemannian manifolds," *Int. J. Bifurcation and Chaos* **11**(9), 2305–2315.
- Sakurai, J. J. [1994] *Modern Quantum Mechanics* Revised edition. (Addison-Wesley, Reading, MA).
- Strogatz, S. H. [1994] *Nonlinear Dynamics and Chaos* (Addison-Wesley, Reading, MA).
- Temam, R. [1997] *Infinite-Dimensional Dynamical Systems in Mechanics and Physics*, Applied Mathematical Sciences, Vol. 68, 2nd edition (Springer-Verlag, NY).
- Wiggins, S. [1990] *Introduction to Applied Nonlinear Dynamical Systems and Chaos*, Texts in Applied Mathematics, Vol. 2 (Springer-Verlag, NY).
- Zwanziger, J. W., Koenig, M. & Pines, A. [1990] "Berry's phase," *Ann. Rev. Phys. Chem.* **41**, 601–646.